JVSTB
JOURNAL OF VACUUM SCIENCE AND TECHNOLOGY B

Understanding the effects of photoacid distribution homogeneity and diffusivity on critical dimension control and line edge roughness in chemically amplified resists

Cheng-Tsung Lee, Richard A. Lawson, and Clifford L. Henderson

Citation: J. Vac. Sci. Technol. B **26**, 2276 (2008); doi: 10.1116/1.2976601
View online: http://dx.doi.org/10.1116/1.2976601
View Table of Contents: http://avspublications.org/resource/1/JVTBD9/v26/i6
Published by the AVS: Science & Technology of Materials, Interfaces, and Processing

Related Articles

Comparison of the effects of downstream H2- and O2-based plasmas on the removal of photoresist, silicon, and silicon nitride
J. Vac. Sci. Technol. B 31, 021206 (2013)

Impacts of point spread function accuracy on patterning prediction and proximity effect correction in low-voltage electron-beam–direct-write lithography
J. Vac. Sci. Technol. B 31, 021605 (2013)

Origin of defects on targets used to make extreme ultraviolet mask blanks
J. Vac. Sci. Technol. A 31, 021403 (2013)

Nanometer scale high-aspect-ratio trench etching at controllable angles using ballistic reactive ion etching
J. Vac. Sci. Technol. B 31, 010604 (2013)

Influence of secondary electrons in high-energy electron beam lithography
J. Vac. Sci. Technol. B 31, 011605 (2013)

Additional information on J. Vac. Sci. Technol. B

Journal Homepage: http://avspublications.org/jvstb
Journal Information: http://avspublications.org/jvstb/about/about_the_journal
Top downloads: http://avspublications.org/jvstb/top_20_most_downloaded
Information for Authors: http://avspublications.org/jvstb/authors/information_for_contributors

ADVERTISEMENT

Complete Dry Vacuum Pump Station
for only **$4995** — HiCube™ Eco
800-248-8254 | www.pfeiffer-vacuum.com

Downloaded 28 Mar 2013 to 130.207.50.120. Redistribution subject to AVS license or copyright; see http://avspublications.org/jvstb/about/rights_and_permissions

Understanding the effects of photoacid distribution homogeneity and diffusivity on critical dimension control and line edge roughness in chemically amplified resists

Cheng-Tsung Lee, Richard A. Lawson, and Clifford L. Henderson[a)]
School of Chemical and Biomolecular Engineering, Georgia Institute of Technology, Atlanta, Georgia 30332-0100

(Received 25 June 2008; accepted 28 July 2008; published 1 December 2008)

Resist critical dimension (CD) control and line edge roughness (LER) reduction has been one of the most challenging issues for sub-100 nm feature patterning in integrated circuit manufacturing. Among those factors dominating CD and LER, photoacid distribution homogeneity and diffusivity are major elements which are correlated to resist material design and have a direct impact on the lithography performance. In this work, a mesoscale stochastic model has been applied to investigate the joint effect of photoacid distribution homogeneity and diffusivity on resist lithography performance. Simulation results suggest that the high photoacid generator (PAG) loading and low photoacid diffusivity provided by polymer bound-PAG resist systems can provide superior lithography performance as compared to traditional blended-PAG resists, which is in good agreement with our previous experimental characterization of polymer bound-PAG resists. The results also suggest that resist image blur is proportional to the square root of the product of photoacid concentration generated at the line edge and the photoacid diffusion coefficient. LER was observed to be proportional to the product of the standard deviation of the extent of deprotection along the nominal line edge and the reciprocal of the gradient of the deprotection profile along the resist line edge. © *2008 American Vacuum Society.* [DOI: 10.1116/1.2976601]

I. INTRODUCTION

Advancements in microlithographic technology have made possible the fabrication of modern integrated circuit (IC) devices with dramatically decreasing feature sizes, increasing device densities, and increasing device speeds for more than four decades. This progress in lithography technology has been achieved by advancements in both lithography equipment and photoresist materials. In the area of lithography tools, state-of-art 193 nm exposure technologies (e.g., immersion lithography and double patterning) have extended the patterning capability of 193 nm optical systems for several semiconductor technology nodes (i.e., 90 nm, 65 nm, and 45 nm) and exhibit the potential for patterning features with sub-40 nm resolution.[1–4] Lithographic tools with shorter wavelength radiation sources, such as extreme ultraviolet lithography, have demonstrated stable progress and will likely be required for sub-32 nm resolution mass production.[5–7] Despite substantial progress in this area of lithography equipment, successful implementation of such lithography technologies still requires resist materials that are capable of translating the aerial image obtained using such exposure tools and processes into a satisfactory physical relief image on the semiconductor substrate. It is this second area, the design and the production of resist materials with the requisite sensitivities, resolutions, and edge roughness performance to meet the stated requirements for future IC technology nodes that is still in some doubt.

The introduction and extensive development of chemically amplified resists (CARs) have continuously provided resist materials with adequate lithography performance for each succeeding IC technology node for more than two decades.[8,9] A typical CAR is a multicomponent blended material consisting of a photoacid generator (PAG), a protected polymer resin, and an optional base quencher. The PAG serves as a photoactive molecule which absorbs the exposure energy provided by the lithography tool and generates a photoacid. The photoacid serves as a chemical amplification element that switches the solubility of the polymer resin. In positive-tone CARs, this occurs via a thermally induced acid-catalyzed deprotection reaction that changes the polarity of the resist polymer. The physical resist image is then formed during a development process which removes the unexposed or exposed region of the resist depending on the tone of the process. While attempting to further extend CARs for sub-50 nm patterning with satisfactory lithography performance, i.e., small critical dimension (CD), fast photospeed, and low line edge or line width roughness (LER or LWR), the blended nature of the traditional CAR platform results in a trilateral tradeoff between these important performance metrics.[10,11] The relatively low PAG loadings possible in such blended resist systems, due generally to low solubilities for traditional PAGs in the resist solutions, often lead to the requirement that the photoacid diffusivity be relatively high, i.e., long catalytic chain length, in order to achieve high photospeeds. However, high photoacid diffusivity causes resist image blur and decreases the achievable resolution. Base additives may be applied to help confine photoacid diffusion and blur at the latent image line edge, but the base in the

[a)]Author to whom correspondence should be addressed; Electronic mail: cliff.henderson@chbe.gatech.edu

Downloaded 28 Mar 2013 to 130.207.50.120. Redistribution subject to AVS license or copyright; see http://avspublications.org/jvstb/about/rights_and_permissions

desired exposed region of the resist can also neutralize photoacid in that region as well which results in reduced photospeed and may actually contribute to increasing the LER/LWR.

Polymer bound-PAG resist systems have been designed and demonstrated which improve CAR lithography performance by directly binding the PAG anion into the polymer main chain.[12] These resist platforms allow for the control and reduction of photoacid diffusivity to reduce diffusion-induced image blur while maintaining desirable high photospeeds by improving the maximum possible PAG loadings that can be used in the resist formulation. The polymer bound PAG resists also have demonstrated larger resist process windows, i.e., exposure and focal latitudes, than their blended-PAG analogs.[13] Although the polymer-bound PAG resists have experimentally demonstrated superior lithography performance as compared to analogous traditional blended-PAG resists, a more detailed understanding of the joint effects of high PAG loading and low photoacid diffusivity on the lithography performance in such materials is still lacking. The goal of the work reported in this article was to develop and utilize a mesoscale resist model to better understand the origins of the observed performance improvement in such resists.

II. MODEL DESCRIPTION

A. Mesoscale resist model

In this work, a resist processing simulation framework has been developed to investigate the correlation between resist properties and the lithography performance. A mesoscale resist model is applied to simulate the exposure and postexposure bake (PEB) processes of a resist film.[14] The resist model is built using a two-dimensional lattice containing 140 $\times 200$ square cells ($x=140$, $y=200$) to represent the top-down image of the resist film. The edge length l of each cell is set as 1.0 nm to represent the approximate volume occupied by a single resin monomer or a photoacid in typical CAR resist films.

B. Modeling initiation

In the beginning of a simulation, an aerial image intensity profile $I(x)$ representing a 70 nm line feature is generated along the x axis according to a sigmoid function described in Eq. (1),

$$I(x) = \frac{1}{1+e^{-\alpha(x-x_L)}} - \frac{1}{1+e^{-\alpha(x-x_R)}}. \tag{1}$$

Here α is the threshold likelihood of the intensity profile and x_L and x_R are the left and right edges of the line image, respectively. For a given α and a nominal CD ($\mathrm{CD_{Nom}}=x_R-x_L$), the normalized image log slope NILS is calculated by Eq. (2),

$$\mathrm{NILS} = w\frac{1}{I(x)}\frac{dI(x)}{dx} = \frac{\mathrm{CD_{Nom}}\alpha}{2}. \tag{2}$$

The probability of finding a PAG in a cell can be assumed to follow the Poisson distribution and can be represented by the average initial PAG loading ratio (mol %) P_{PAG} of the resist. The probability of converting a PAG into a photoacid can also be assumed to follow the Poisson distribution and is determined using first-order photodecomposition kinetics.[15] For a given photoacid generation rate constant C, exposure intensity $I(x)$, and exposure time t of a cell position (x,y), the joint probability of generating a photoacid at the cell $P_{\mathrm{acid}}(x,y)$ is determined by Eq. (3),

$$P_{\mathrm{acid}}(x,y) = P_{\mathrm{PAG}}[1-e^{-\mathrm{C}I(x,y)t}]. \tag{3}$$

Photoacids are first assigned to the lattice according to Eqs. (1) and (3). The remaining cells are then filled with protected resist monomers to complete the exposed resist model initiation for a positive-tone resist.

C. Photoacid diffusion

A Monte Carlo stochastic process is applied to describe the random walk nature of photoacid diffusion behavior during the PEB process.[14] Given an effective diffusion coefficient D_{eff} to represent the diffusivity of photoacids in the resist film, the required step time τ for a photoacid to move from one cell to another adjacent cell can be described by Eq. (4).

$$D_{\mathrm{eff}} = \frac{l^2}{2d\tau}. \tag{4}$$

Here d is the dimensionality of the lattice. Photoacids are allowed to randomly move from their original cells to adjacent cells in the two-dimensional lattice. A diagonal movement is not allowed for simplification. A periodic boundary condition is applied to the lattice to approximate a dense line pattern. In principle a larger D_{eff} gives a smaller τ for a photoacid molecule to move one cell distance. A photoacid with higher diffusivity can make more moves within a certain PEB time and thus exhibits a larger diffusion length.

D. Deprotection and development

A diffusion-limited assumption is applied in this work to describe the reaction-diffusion process during PEB since the time scale of photoacid diffusion is significantly larger than the time scale of the photoacid catalytic reaction in typical CARs.[16] The deprotection reaction occurs immediately when a photoacid moves to a protected cell in the simulation. For every set of initial photoacid distributions, the model is repeated 100 times and an average deprotection probability of each cell after PEB is calculated. On the length scale relevant to LER of interest in this work (i.e., several tens of nanometers, corresponding to low-spatial frequency LER), a simple threshold or infinite contrast development model was used to predict the resist profile after development. A monomer is removed if its protection probability is lower than a threshold

Downloaded 28 Mar 2013 to 130.207.50.120. Redistribution subject to AVS license or copyright; see http://avspublications.org/jvstb/about/rights_and_permissions

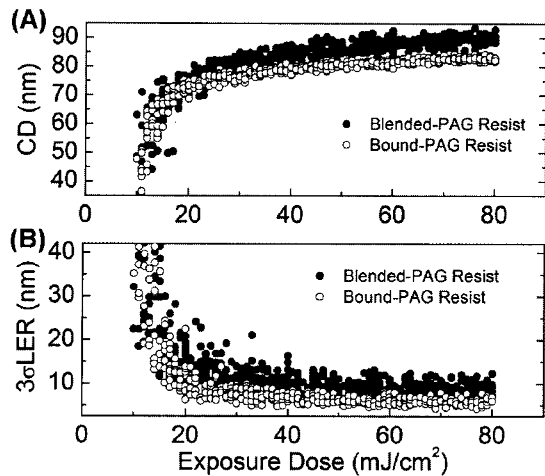

FIG. 1. Effect of exposure dose on (A) space CD and (B) LER of the polymer-bound PAG and blended PAG resist models under the same NILS.

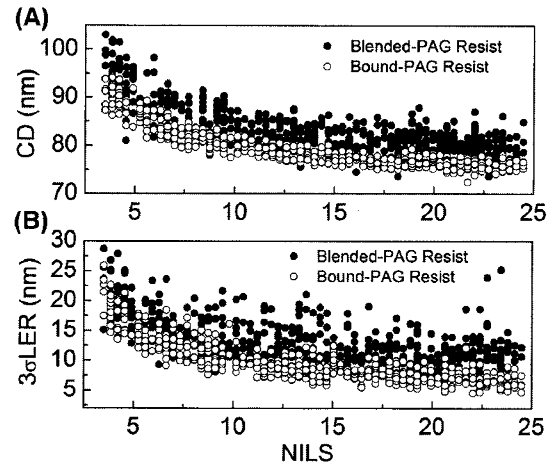

FIG. 2. Effect of NILS on (A) space CD and (B) LER of both resist models under the same exposure dose.

value (0.5) and a final resist profile is obtained. The resist line edge and thus the space CD and low-spatial frequency LER are determined.

III. RESULTS AND DISCUSSION

A. Exposure dose and aerial image quality effects

Two resist models were built in this work to represent the approximate behavior of both polymer bound PAG and the traditional blended-PAG resists. The *bound-PAG* resist has high PAG loading (10.0 mol %) and low photoacid diffusivity ($0.07\ \mathrm{nm}^2/\mathrm{s}$), while the *blended-PAG* resist has low PAG loading (2.0 mol %) and high photoacid diffusivity ($0.5\ \mathrm{nm}^2/\mathrm{s}$). The same Dill C parameter value of $0.04\ \mathrm{cm}^2/\mathrm{mJ}$ was used in the simulation for both resist models. The two resist models were designed to have the same sizing dose ($\mathrm{CD_{Nom}}=70$ nm at $17\ \mathrm{mJ/cm}^2$) under the same NILS (=17.5) to represent two resists with equal photospeed for the nominally 70 nm features used in the rest of the simulations. The effective diffusion coefficients for these two resists were selected simply to mimic the fact that the bound photoacid should, in general, have a lower diffusion coefficient than an analogous photoacid generated from a blended PAG, with the specific values being estimated from measurements internally of photoacid diffusion coefficients from various resist systems. Since the data collected so far suggested a range of possible diffusion coefficients for various photoacids (i.e., both bound and unbound) in different resist systems, the exact values were chosen to again maintain the same photospeed in the two model resists at the different PAG loadings used in models. As shown in Fig. 1, both resists show that space CD increases and LER decreases as exposure dose increases and ultimately both plateau at high doses. However, the bound-PAG resist shows less increase and fluctuation of space CD and LER than the blended-PAG resist. By taking $\pm 10\%$ of the $\mathrm{CD_{Nom}}$ as the maximum allowable CD error and calculating the exposure latitude EL, the bound-PAG resist shows more than 2.5 times larger EL (112%) than the blended-PAG resist (47%). The bound-PAG resist also showed at least 50% improvement of LER of the blended-PAG resist at the exposure doses analyzed. The effects of NILS on space CD and LER of both resist models under the same exposure dose ($30\ \mathrm{mJ/cm}^2$) are shown in Fig. 2. Both resist models show the increase in space CD and LER upon NILS decrease, however, the bound-PAG resist maintains lower CD error and LER, as well as less CD and LER fluctuations than the blended-PAG resist. From the maximum to the minimum NILS tested in this work, the bound-PAG resist shows less space CD increase (18.9%) than the blended-PAG resist (20.7%). The bound-PAG resist also shows less 3σ LER increase (16.3 nm) than the blended-PAG resist (19.4 nm). These trends in the simulation results are in good agreement with our previous experimental characterization of polymer-bound PAG resists.[12,13]

B. Scaling factors of CD variation and LER

Resist CD variation (ΔCD, relative to $\mathrm{CD_{Nom}}$) has been correlated to exposure dose and photoacid diffusivity during the PEB process.[11,16,17] By calculating ΔCD and the corresponding root mean square of the product of photoacid number generated beyond the aerial image line edge ($n_{\mathrm{acid,edge}}$ toward the unexposed region) and photoacid diffusivity, the results of the two different resist models under different exposure doses are plotted in Fig. 4(a). A global linear relationship between these two factors is found in both resists, and the observed resist CD variation can be well scaled as shown in Eq. (5). This correlation indicates that the increased space CD upon exposure dose increase in the positive-tone resists is mainly due to the coupling effect of the increase in photoacid concentration at the aerial image line edge and their diffusivity,

$$\Delta\mathrm{CD} \propto \sqrt{n_{\mathrm{acid,edge}} D_{\mathrm{eff}}}. \tag{5}$$

Resist CD fluctuation and LER have been theoretically and experimentally proven to originate from a number of statistical fluctuation effects, such as originating from the expo-

Downloaded 28 Mar 2013 to 130.207.50.120. Redistribution subject to AVS license or copyright; see http://avspublications.org/jvstb/about/rights_and_permissions

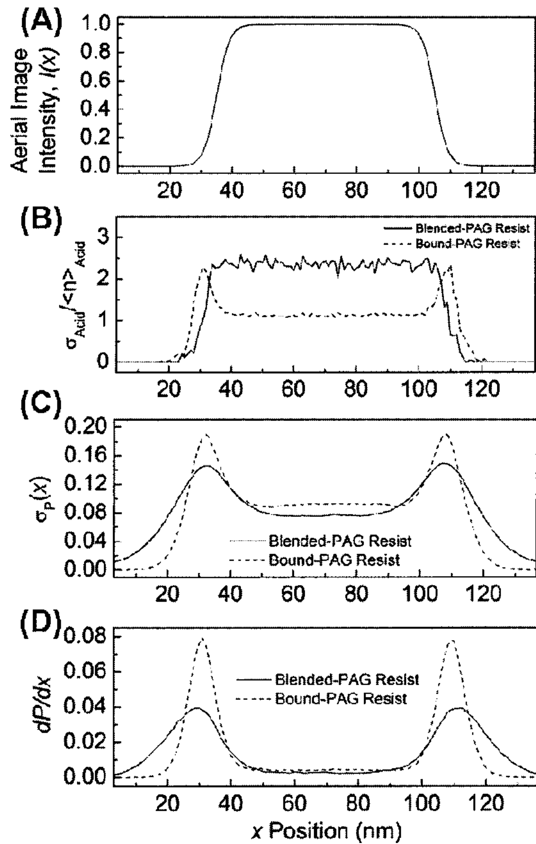

FIG. 3. Lateral distribution of (A) the fractional uncertainty of photoacid number, (B) the standard deviation of resist deprotection, and (C) the resist derotection gradient of both resist models under the same exposure dose and NILS.

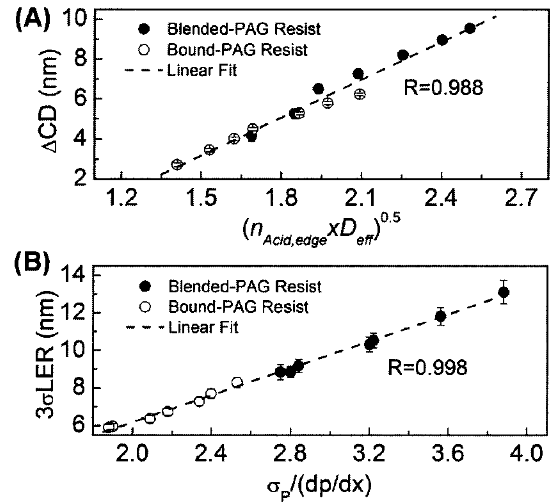

FIG. 4. The correlations between (A) space CD variation and photoacid number (or concentration) and diffusivity and (B) LER and resist deprotection profile.

sure, resist physicochemistry and postexposure processing.[11,18–20] The effects caused by the resist physicochemistry are resist deprotection homogeneity and gradient at the line edge after PEB and are the direct consequence of initial photoacid distribution homogeneity and photoacid diffusivity. By calculating the number of photoacids in a resist volume (an 11×1 cell region in this work), a fractional uncertainty of the number of photoacids U_{acid} of all the investigated resist volumes can be defined, as shown in Eq. (6), and can be used to determine the photoacid distribution homogeneity,

$$U_{\mathrm{acid}} = \sigma_{\mathrm{acid}} / \langle n_{\mathrm{acid}} \rangle . \quad (6)$$

Here σ_{acid} and $\langle n_{\mathrm{acid}} \rangle$ are the standard deviation and the average of the photoacid number of all investigated resist volumes, respectively. A low value of U_{acid} indicates a high photoacid distribution homogeneity and vice versa. Under the same aerial image intensity profile as shown in Fig. 3(a), the uncertainty of photoacids of both resists along the x-axis under the same exposure dose ($40\ \mathrm{mJ/cm^2}$) is shown in Fig. 3(b). A fivefold higher PAG loading of the bound-PAG resist provides a 60% lower U_{acid} at the bulk exposure region than the blended-PAG resist. However, at the aerial image line edge where the CD fluctuation and LER actually occur, the decrease in exposure dose also causes the decrease in photoacids and thus increases U_{acid} of the bound-PAG resist comparable to the blended-PAG resist. Obviously the initial photoacid distribution only is not sufficient to evaluate resist CD fluctuation and LER since both resist models have high U_{acid} at the aerial image line edge. The diffusion of photoacids during the PEB may also enhance or smooth the fluctuation caused by initial photoacid distribution. A combinatorial effect of photoacid distribution and diffusivity is essential for a better evaluation of CD fluctuation and LER. Figures 3(c) and 3(d) show the standard deviation σ_P and the gradient dP/dx of the resist deprotection profile along the x-axis after PEB. The effect of the initial photoacid distribution heterogeneity at the line edge of the blended-PAG resist is smoothed out to a large degree due to high photoacid diffusivity and leads to a lower σ_P than the bound-PAG resist. However, the high photoacid diffusivity of the blended-PAG resist also reduces the deprotection gradient at the line edge and leads to a lower resist contrast than the bound-PAG resist. Resist deprotection gradient has been proven to have a direction impact on LER.[17] By plotting 3σ LER and the corresponding $\sigma_P/(dP/dx)$ of both resist models as shown in Fig. 4(b), a global linear relationship is found between these two factors with excellent correlation, and LER can be well scaled by the resist deprotection profile as indicated in Eq. (7). These results indicate that although high PAG loading of the bound-PAG resist may not improve initial photoacid distribution homogeneity after exposure and resist deprotection homogeneity at the line edge under the conditions simulated, the low photoacid diffusivity of the bound-PAG resist can increase resist deprotection gradient at the line edge which is equivalent to an effectively higher resist contrast at the line edge, thus improving the resist CD fluctuations and reducing LER,

$$\mathrm{LER} \propto \frac{\sigma_P}{dP/dx} . \quad (7)$$

Downloaded 28 Mar 2013 to 130.207.50.120. Redistribution subject to AVS license or copyright; see http://avspublications.org/jvstb/about/rights_and_permissions

IV. CONCLUSIONS

In conclusion, the effects of exposure dose and aerial image quality on two resist models, one representing a polymer-bound PAG resist and one representing a blended PAG resist, have been investigated via a mesoscale stochastic simulation. The bound-PAG resist, which possesses higher PAG loading and low photoacid diffusivity, shows superior resist CD control, lower LER, and a larger process window than the analogous blended-PAG resist with relatively low PAG loading and high photoacid diffusivity. The trends of the simulation results are in good agreement with our previous experimental characterization of the polymer bound-PAG resists. The results also suggest that resist CD variation can be well scaled by the root mean square of the product of photoacid number or concentration at the line edge and its diffusivity. Likewise, resist LER can be well scaled by the standard deviation of resist deprotection divided by its gradient at the line edge. The improved lithography performance of the polymer-bound PAG resist under the conditions simulated in this work as compared to a traditional blended PAG resist is observed to be due to a coupled effect arising from both the higher PAG loading possible in the polymer-bound PAG material and the reduced photoacid diffusivity. The combination of these two factors allows for the production of a polymer-bound PAG resist with a higher effective chemical contrast at the line edge than the analogous blended PAG resist while maintaining the same nominal photospeed.

ACKNOWLEDGMENTS

The authors would like to gratefully acknowledge Intel Corporation for research funding support. The authors would also like to thank Dr. Wang Yueh, Dr. Todd Younkin, Dr. Steve Putna, and Dr. Jeanette Roberts at Intel for their contributions and helpful discussions related to this work.

[1]B. J. Lin, J. Microlithogr., Microfabr., Microsyst. **1**, 7 (2002).
[2]B. J. Lin, Proc. SPIE **5377**, 46 (2004).
[3]S. Hsu, J. Park, D. V. D. Broeke, and J. F. Chen, Proc. SPIE **5992**, 59921Q (2006).
[4]J. Finders, M. Dusa, B. Vleeming, H. Megens, B. Hepp, M. Maenhoudt, S. Cheng, and T. Vandeweyer, Proc. SPIE **6924**, 692408 (2008).
[5]C. W. Gwyn, R. Stulen, D. Sweeney, and D. Attwood, J. Vac. Sci. Technol. B **16**, 3142 (1998).
[6]B. L. Fontaine *et al.*, J. Vac. Sci. Technol. B **25**, 2089 (2007).
[7]B. Wu and A. Kumar, J. Vac. Sci. Technol. B **25**, 1743 (2007).
[8]H. Ito and C. G. Willson, Polym. Eng. Sci. **23**, 1012 (1983).
[9]H. Ito, Adv. Polym. Sci. **172**, 37 (2005).
[10]R. L. Bristol, Proc. SPIE **6519**, 65190W (2007).
[11]G. M. Gallatin, Proc. SPIE **5754**, 38 (2005).
[12]C.-T. Lee, C. L. Henderson, M. Wang, K. E. Gonsalves, and W. Yueh, J. Vac. Sci. Technol. B **25**, 2136 (2007).
[13]C.-T. Lee, M. Wang, K. E. Gonsalves, and C. L. Henderson (unpublished).
[14]J. J. Biafore, M. D. Smith, S. A. Robertson, and T. Graves, Proc. SPIE **6519**, 65190Y (2007).
[15]F. H. Dill, W. P. Hornberger, P. S. Hauge, and J. M. Shaw, IEEE Trans. Electron Devices **22**, 445 (1975).
[16]F. A. Houle, W. D. Hinsberg, M. I. Sanchez, and J. A. Hoffnagle, J. Vac. Sci. Technol. B **20**, 924 (2002).
[17]T. Kawakami, T. Nagai, Y. Nishimura, M. Shima, S. Kusumoto, and T. Shimokawa, Proc. SPIE **6519**, 65193K (2007).
[18]A. R. Pawloski, A. Acheta, H. J. Levinson, T. B. Michaelson, A. Jamieson, Y. Nishimura, and C. G. Willson, J. Microlithogr., Microfabr., Microsyst. **5**, 1 (2006).
[19]Q. Lin, R. Sooriyakumaran, and W.-S. Huang, Proc. SPIE **3999**, 230 (2000).
[20]M. Ercken, L. H. A. Leunissen, I. Pollentier, G. P. Patsis, V. Constantoudis, and E. Gogolides, Proc. SPIE **5375**, 266 (2004).

Downloaded 28 Mar 2013 to 130.207.50.120. Redistribution subject to AVS license or copyright; see http://avspublications.org/jvstb/about/rights_and_permissions